Extending the Numerov Process to the Semiconductor Transport Equations

Nicolò Speciale, Rossella Brunetti[1], Massimo Rudan
"E. De Castro" Advanced Research Center on Electronic Systems (ARCES) and Department DEI
University of Bologna, Viale Risorgimento 2, I-40136 Bologna, Italy
nicolo.speciale(massimo.rudan)@unibo.it
[1]*FIM Department, University of Modena and Reggio Emilia, Via Campi 213/A, I-41125 Modena, Italy*
rossella.brunetti@unimore.it

***Abstract*—Some classes of differential equations are amenable to a numerical solution based on the Numerov process (NP), whose accuracy can be up to two orders of magnitude superior with respect to the standard finite-difference or box-integration methods, with a negligible increase in the computational cost. The paper shows that the equations describing charge transport in solid-state devices can suitably be manipulated to make the application of NP possible. Also, thanks to a specifically-tailored algebraic solver, the 1D Poisson equation is fully decoupled from the transport equation, this reducing the procedure to the solution of a single non-linear equation. The example of an Ovonic device is considered, used as selector in phase-change memory applications.**

***Index Terms*—Numerov Process, Transport equations**

I. Introduction

A differential equation of the second order where the first derivative of the unknown function $z(x)$ is missing: $-z'' = Q(x)\,z + P(x)$, is amenable to a discretization scheme based on the Numerov process (NP), whose accuracy is $\mathrm{O}(h^4)$, with h the grid size, in contrast to $\mathrm{O}(h^2)$ of the standard methods (details in [1] and references therein). Although the original version of NP applies to a uniform grid, this constraint can be relieved as shown below. Letting $Q = 0$, the above equation yields the Poisson equation, with $z = u$ the normalized electric potential and $P = q/(\varepsilon\, k_B\, T)\,\varrho$, where ϱ is the charge density; if, instead, one lets $P = 0$, the time-independent Schrödinger equation is found, with $z = w$ the spatial part of the wave function and $Q = 2\,m\,(E - V)/\hbar^2$, where E and $V(x)$ are the total and potential energy, respectively. Due to the superior performance of NP with respect to the standard finite-difference method, it is of interest to seek for extensions of NP to other classes of equations; among these, those that model charge transport in solid-state devices.

II. The Model Equations

Referring to the semiclassical model for charge transport in solids, a one-dimensional case with only one type of carriers, e.g., electrons, is considered. This situation is typical, among others, of devices like phase-change memories (e.g., [2] and references therein); the form of the Poisson equation thus becomes $u'' = u''(n, n_T)$, with n, n_T the concentrations of electrons and empty traps, respectively. Combining the steady-state continuity equation for the electrons, $J_n' = q\,U$, with the transport equation of the drift-diffusion form, $J_n = q\,D_n\,(n' - u'\,n)$, yields $n'' - u'\,n' - u''\,n = U/D_n$, where $U = U(n, n_T)$ is the net-recombination rate and $D_n = \text{const}$ the diffusion coefficient of the electrons. In a decoupled solution scheme, $-u'' = q/(\varepsilon\, k_B\, T)\,\varrho = P(n, n_T)$ plays in the latter equation the role of a coefficient known from the previous iteration. Letting $s = -(U/D_n)\,\exp(-u/2)$, $g = n\,\exp(-u/2)$, the equation is given a form suitable for the application of NP:

$$-g'' = c\,g + s\,, \qquad c = P/2 - (u')^2/4\,. \tag{1}$$

Note that the transformation leading to (1) is not a reduction to the self-adjoint form, which would in fact read $[n'\,\exp(-u)]' = (U/D_n - P\,n)\,\exp(-u)$, nor an exponential fitting like the one typically adopted for solving the semiconductor equations, which would read $q\,D_n\,[n\,\exp(-u)]' = J_n\,\exp(-u)$ with $J_n = \text{const}$ over the segment connecting two nodes (the exponential-fitting scheme is also known as *Scharfetter-Gummel method* [3]).

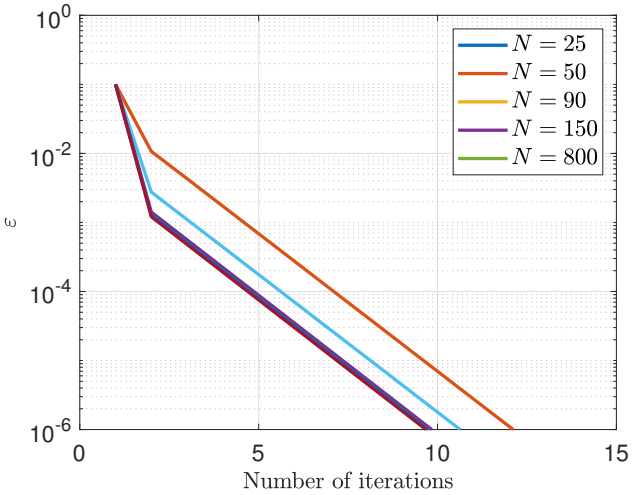

Fig. 1. Error ϵ vs. the number of iterations, with $V = 0.1$ V applied bias. The legend shows the number of nodes of each run.

978-1-7281-0940-4/19/$31.00 ©2019 IEEE

III. The Numerov Process

Given a uniform grid having N internal nodes with an element size equal to h, application of NP to the Poisson equation yields the algebraic system

$$-u_{i-1} + 2\,u_i - u_{i+1} = \frac{h^2}{12}\,(P_{i-1} + 10\,P_i + P_{i+1})\,, \quad (2)$$

while its application to (1) yields the algebraic system

$$-\left(1 + \frac{h^2}{12}\,c_{i-1}\right)\,g_{i-1} + \left(2 - 10\,\frac{h^2}{12}\,c_i\right)\,g_i \quad (3)$$

$$-\left(1 + \frac{h^2}{12}\,c_{i+1}\right)\,g_{i+1} = \frac{h^2}{12}\,(s_{i-1} + 10\,s_i + s_{i+1})\,.$$

The unknowns of (3) are the nodal values $g_i = n_i\,\exp(-u_i/2)$, whereas c_i and s_i depend on the original unknown n through P and U. If the nodal values of $\exp(-u/2)$ are incorporated as they are into the coefficients of (3), the matrix may become stiff; it is preferable to restore the original unknown by multiplying both sides of (3) by $\exp(u_i/2)$. The new form of (3) thus obtained is more convenient because the potential differences between neighboring nodes appear, instead of the nodal potential alone. For instance, g_{i-1} is replaced with $n_{i-1}\,\exp[(u_i - u_{i-1})/2]$, and so on. Finally, one must express u' in the second relation of (1); using again NP, one easily finds

$$u'_i = \frac{u_{i+1} - u_{i-1}}{2\,h} + h\,\frac{P_{i+1} - P_{i-1}}{12}\,. \quad (4)$$

When $i = 2, \ldots N-1$, (4) involves only the internal nodes; when $i = 1$ or $i = N$, (4) involves one or the other boundary condition (u_0 and $P_0 = 0$ or, respectively, u_{N+1} and $P_{N+1} = 0$); finally, when $i = 0$ or $i = N+1$, (4) involves the potential and charge inside the contacts; as the latter are equipotential and neutral, one finds $u_{-1} = u_0$, $P_{-1} = 0$ and $u_{N+2} = u_{N+1}$, $P_{N+2} = 0$. By the same token one finds

$$g'_i = \frac{(6 + h^2\,c_{i+1})\,g_{i+1} - (6 + h^2\,c_{i-1})\,g_{i-1}}{12\,h} + \\ + h\,\frac{s_{i+1} - s_{i-1}}{12}\,. \quad (5)$$

IV. Fully Decoupling the Model Equations

As the coefficients of (3) depend on the nodal values u_i of the electric potential, it is necessary to iterate between the solution of (3) and that of the algebraic system deriving from the Poisson equation. In general such solutions are obtained by algebraic solvers that provide the nodal values in a prescribed sequence; considering for instance the $\boldsymbol{A} = \boldsymbol{L}\,\boldsymbol{U}$ decomposition, one obtains the ith nodal value of the potential only after calculating it at nodes 1 through $i-1$ (or at nodes N through $i+1$). A neater approach would be that in which u_i is obtained as soon as necessary, without the need of calculating the rest of the sequence; such a result is indeed achieved for the 1D Poisson equation of the form (2) by the method shown in [4, p. 769], having the advantage that each nodal value u_i can be calculated independently of the others; in fact, using the short-hand notation C_i for the right hand side of (2), and letting

$$Z_j = h^2\,\sum_{k=1}^{j} C_k\,, \quad Y_i = \sum_{j=1}^{i} Z_j\,, \quad i = 1\,\ldots\,N\,, \quad (6)$$

and $R = (u_{N+1} - u_0 + Y_N)/(N+1)$, one finds $u_1 = u_0 + R$,

$$u_i = u_0 + i\,R - Y_{i-1}\,, \qquad i = 2\,\ldots\,N\,. \quad (7)$$

The potential differences that appear in (3) are easily evaluated from (6–7):

$$u_i - u_{i-1} = R - Z_{i-1}\,, \quad u_{i+1} - u_{i-1} = 2\,R - Z_{i-1} - Z_i\,.$$

If the discretized form of the Poisson equation is such that the method based on (6–7) is applicable, the calculation is cheaper than the $\boldsymbol{A} = \boldsymbol{L}\,\boldsymbol{U}$ decomposition and completely decouples the transport equation from the Poisson equation.

It is also worth remarking other differences with respect to the standard discretization schemes: here, after discretization, all functions and derivatives belong to the nodes, whereas in the standard schemes the functions and the even derivatives belong to the nodes, while the odd derivatives belong (in one dimension) to the elements. Also, no hypothesis is necessary here about the behavior of the discretized functions along each element.

V. Stability

Iterations are in general necessary due to the non-linearity of the equations; for instance, in a semiconductor the normalized charge concentrations P_{i-1}, P_i, P_{i+1} that appear at the right hand side of (2) depend on the unknown u either exponentially or through a Fermi integral; in both cases, the derivatives $\mathrm{d}P_i/\mathrm{d}u$ are negative irrespective of the fact that electrons or holes are considered: in fact, hole concentration contributes positively to the charge density, and decreases with increasing u; electron concentration contributes negatively, and increases with increasing u. It follows that the extra terms obtained from the linearization with respect to u add weight to the main diagonal of the algebraic system (2), thereby improving convergence.

Coming now to (3), when the expressions of c_{i-1}, c_i, c_{i+1} that appear in the second equation of (1) are inserted into (3), the right hand side of the ith row of the resulting algebraic system is the sum of three terms: the first one, $A_i = -g_{i-1} + 2\,g_i - g_{i+1}$, has the same structure as that of the discretized Poisson equations (2). The other two terms read

$$B_i = \frac{(u'_{i-1})^2\,g_{i-1} + 10\,(u'_i)^2\,g_i + (u'_{i+1})^2\,g_{i+1}}{48/h^2}\,, \quad (8)$$

$$C_i = -\frac{P_{i-1}\,g_{i-1} + 10\,P_i\,g_i + P_{i+1}\,g_{i+1}}{24/h^2}\,. \quad (9)$$

As the coefficients in (8) are non negative, they add weight to all diagonals of the algebraic system (3); due to factor 10, the added weight of the main diagonal is dominant unless the ith node is in an extremum of u. As for (9), the analysis is

complicated by the presence of the normalized charge density P, which may have either sign. On the other hand, (9) is of order 2 in h, whereas, due to a cancellation (compare with (4)), B_i is of the same order as A_i, namely, order 0.

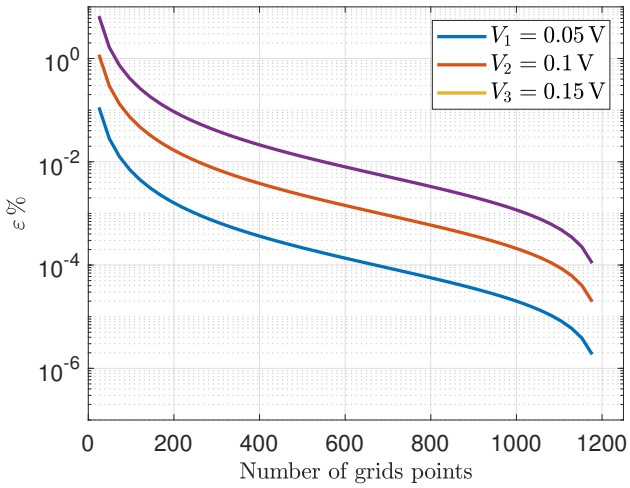

Fig. 2. Maximum error (in percentage) of the node values between the reference solution ($N = 2000$) and different runs for different biases ($V_1 = 0.05\,\mathrm{V}$, $V_2 = 0.1\,\mathrm{V}$, and $V_3 = 0.15\,\mathrm{V}$).

VI. Results

The scheme for solving the transport model was applied here to a chalcogenide layer of thickness $L = 30$ nm and a Gaussian trap distribution in the direction of the external field. Uniformity was assumed in the direction normal to the field, and the applied bias V was kept below threshold. The analysis was carried out on different grids: we started with a large number of nodes (reference solution: $N = 2000$) and decreased it down to $N = 25$. Fig. 1 shows $\epsilon = \max_i(|n_i^{\mathrm{new}} - n_i^{\mathrm{old}}|/n_i^{\mathrm{old}})$ vs. the number of iterations at different values of N, with $V = 0.1$ V applied bias. The convergence criterion was $\epsilon \leq 10^{-6}$. Letting $C(N)$ be the computational cost needed to fulfill this convergence criterion, the analysis showed that $C(1500) \simeq 26 \times C(25)$. To measure the accuracy of different solutions as function of N, the relative error was calculated in corrispondence of all nodes of the coarser grid ($N = 25$) by considering the difference between the values of the solution for all N with respect to the reference solution. Fig. 2 compares the maximum difference (in percentage) for different biases.

Next, the error of the present method has been compared with that of the exponential-fitting one; the results are shown in the Tables. As before, the starting point was a reference solution obtained with a dense grid ($N = 2000$); then, other solutions were run with a progressively-decreasing number of nodes, and the maximum difference with respect to the reference solution was extracted. More precisely, Tab. I lists $\eta(\varphi) = \max_i|\varphi_i - \varphi_i^{\mathrm{ref}}|$ for different values of the grid nodes and applied bias; the errors of the exponential-fitting method are listed in column "SG". In turn, Tab. II lists $\eta(n) = \max_i|n_i - n_i^{\mathrm{ref}}|/n_M^{\mathrm{ref}}$, with n_M^{ref} the maximum concentration of the reference solution. Despite the simplicity of the problem in hand, the improvement of the present method with respect to the standard one is about one order of magnitude in all cases.

A final check refers to the constancy of the current density; in fact, in a one-dimensional, steady-state case where the mobility of the trapped electrons is set to zero, the continuity equation yields $J_n' = qU = 0$. As remarked above, with the present method all functions and derivatives belong to the nodes: it follows that J_n and $J_n' = q\,D_n\,(n'' - u'\,n' - u''\,n)$ belong to the nodes as well; the latter quantity is shown in Fig. 3 as a function of position.

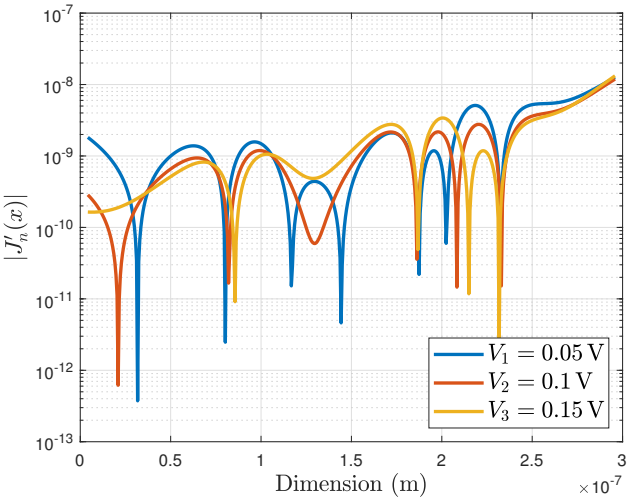

Fig. 3. Modulus $|J_n'|$ as a function of position, with different biases ($V_1 = 0.05\,\mathrm{V}$, $V_2 = 0.1\,\mathrm{V}$, and $V_3 = 0.15\,\mathrm{V}$). The outcome is similar for all grids examined.

To summarize, like in the case of the Schrödinger equation [1], the NP-based approach represents a fairly simple way to improve the solution of the semiconductor equations with a limited increase in the computational burden. Indeed, the drift-diffusion and current-continuity equations have been considered here by way of example; in fact, all pairs of moments of order $2\,k$ and $2\,k+1$, $k = 0, 1, \ldots$ of the Boltzmann transport equation have the same structure: those of even order have the form $-\operatorname{div}\boldsymbol{S} = C$, those of odd order have the form $\boldsymbol{S} = a\,\operatorname{grad}\sigma + \sigma\,\nabla b$, with a suitable meaning of symbols; it follows that the present method applies to any order of transport model in one dimension; also, considering that in the dynamic case the term C above embeds the time derivative $\partial\sigma/\partial t$, the method is not limited to the steady state.

It may be argued that the approach depicted here is applicable only in the one-dimensional case when a uniform grid is used; in fact this is not true: NP has been extended to the variable stepsize, still in one dimension [5]. The applicability to 1D cases is not too severe a constraint when the solution of transport problems in nano-sized cylindrical structures (e.g., nanowires or carbon-nanotube transistors) is sought, where the

typical approach decouples the longitudinal coordinate from the transversal ones [6].

Conversely, the extension of NP to the two- and three-dimensional cases using tensor-product, uniformly-spaced grids has also been achieved (in [7], with reference to the Schrödinger equation), whereas that to non-uniform, multi-dimensional grids is still missing. The multi-dimensional form of (1) is readily obtained with the replacements $g'' \leftarrow \nabla^2 g$ and $u' \leftarrow |\nabla u|$, to find

$$-\nabla^2 g = c\, g + s\,, \qquad c = P/2 - |\nabla u|^2/4\,. \tag{10}$$

Considering the case of a tensor-product, uniformly-spaced grid, the notation becomes awkward even in two dimensions; following [7] we adopt a matrix notation of the form

$$a_{11}\, g_{i+1}^{j-1} + a_{12}\, g_{i+1}^{j} + a_{13}\, g_{i+1}^{j+1} + a_{21}\, g_{i}^{j-1} + \cdots \tag{11}$$
$$+\, a_{23}\, g_{i}^{j+1} + \cdots + a_{33}\, g_{i-1}^{j+1} = \left[\begin{array}{ccc} a_{11} & a_{12} & a_{13} \\ a_{21} & a_{22} & a_{23} \\ a_{31} & a_{32} & a_{33} \end{array}\right]_g ,$$

where the lower (upper) index of $g_i^j\,, \ldots$ refers to the x (y) axis. Application of NP in two dimensions yields, first,

$$\left[\begin{array}{ccc} 1 & 0 & 1 \\ 0 & -4 & 0 \\ 1 & 0 & 1 \end{array}\right]_g = 2\,h^2\,(\nabla^2 g)_i^j + \tag{12}$$
$$+\, \frac{h^4}{6}\,[\nabla^2(\nabla^2 g)]_i^j + \frac{2}{3}\left[\begin{array}{ccc} 1 & -2 & 1 \\ -2 & 4 & -2 \\ 1 & -2 & 1 \end{array}\right]_g .$$

Taking the Laplacian of both sides of (12), and neglecting the 6th-order derivatives, allows one to eliminate $[\nabla^2(\nabla^2 g)]_i^j$. Finally, replacing $(\nabla^2 g)_i^j$ from (10) and letting

$$\boldsymbol{M} = -\left[\begin{array}{ccc} 1 & 4 & 1 \\ 4 & -20 & 4 \\ 1 & 4 & 1 \end{array}\right], \quad \boldsymbol{J} = \left[\begin{array}{ccc} 0 & 0 & 0 \\ 0 & 1 & 0 \\ 0 & 0 & 0 \end{array}\right], \tag{13}$$

eventually yields the two-dimensional generalization of (3):

$$\boldsymbol{M}_g - h^2\left(6\,\boldsymbol{J}_{c\,g} - \frac{\boldsymbol{M}_{c\,g}}{12}\right) = h^2\left(6\,\boldsymbol{J}_s - \frac{\boldsymbol{M}_s}{12}\right). \tag{14}$$

The result expressed by (14) extends that of [7] to the second-order equation of the general form; its derivation also shows that, like in the one-dimensional case, no hypothesis is necessary about the behavior of the discretized functions inside each elements or along its edges.

TABLE I
MAXIMUM ERROR ON THE POTENTIAL $\varphi(x)$

Bias	# of nodes	SG	This work
0.05 V	50	$2.08 \cdot 10^{-05}$	$1.32 \cdot 10^{-06}$
	100	$2.79 \cdot 10^{-06}$	$3.26 \cdot 10^{-07}$
	150	$9.81 \cdot 10^{-06}$	$1.33 \cdot 10^{-07}$
	300	$6.72 \cdot 10^{-08}$	$6.57 \cdot 10^{-09}$
	500	$6.57 \cdot 10^{-08}$	$5.38 \cdot 10^{-09}$
0.1 V	50	$4.08 \cdot 10^{-05}$	$1.25 \cdot 10^{-05}$
	100	$3.74 \cdot 10^{-05}$	$3.00 \cdot 10^{-06}$
	150	$6.01 \cdot 10^{-05}$	$1.22 \cdot 10^{-06}$
	300	$4.97 \cdot 10^{-07}$	$6.13 \cdot 10^{-08}$
	500	$8.14 \cdot 10^{-07}$	$4.92 \cdot 10^{-08}$
0.15 V	50	$2.75 \cdot 10^{-04}$	$5.72 \cdot 10^{-05}$
	100	$3.44 \cdot 10^{-04}$	$1.36 \cdot 10^{-05}$
	150	$4.19 \cdot 10^{-05}$	$5.56 \cdot 10^{-06}$
	300	$2.38 \cdot 10^{-06}$	$2.78 \cdot 10^{-07}$
	500	$2.19 \cdot 10^{-06}$	$2.23 \cdot 10^{-07}$

TABLE II
MAXIMUM ERROR ON THE CONCENTRATION $n(x)$

Bias	# of nodes	SG	This work
0.05 V	50	$3.47 \cdot 10^{-02}$	$5.17 \cdot 10^{-03}$
	100	$2.71 \cdot 10^{-02}$	$1.08 \cdot 10^{-04}$
	150	$2.46 \cdot 10^{-03}$	$1.14 \cdot 10^{-04}$
	300	$3.11 \cdot 10^{-05}$	$5.72 \cdot 10^{-06}$
	500	$2.68 \cdot 10^{-05}$	$1.76 \cdot 10^{-06}$
0.10 V	50	$5.21 \cdot 10^{-02}$	$1.03 \cdot 10^{-02}$
	100	$4.23 \cdot 10^{-02}$	$1.04 \cdot 10^{-03}$
	150	$3.91 \cdot 10^{-03}$	$1.02 \cdot 10^{-03}$
	300	$4.89 \cdot 10^{-04}$	$5.02 \cdot 10^{-05}$
	500	$4.11 \cdot 10^{-04}$	$1.50 \cdot 10^{-05}$
0.15 V	50	$6.34 \cdot 10^{-01}$	$5.48 \cdot 10^{-02}$
	100	$5.17 \cdot 10^{-01}$	$1.45 \cdot 10^{-02}$
	150	$4.77 \cdot 10^{-02}$	$6.03 \cdot 10^{-03}$
	300	$6.02 \cdot 10^{-02}$	$3.05 \cdot 10^{-04}$
	500	$5.17 \cdot 10^{-03}$	$2.15 \cdot 10^{-04}$

REFERENCES

[1] F. Buscemi, E. Piccinini, R. Brunetti, and M. Rudan, "High-Order Solution Scheme for Transport in Low-D Devices," in *IEEE International Conference on Simulation of Semiconductor Processes and Devices (SISPAD)*, Yokohama, September 2014, pp. 161–164.

[2] E. Piccinini, R. Brunetti, and M. Rudan, "Self-Heating Phase-Change Memory-Array Demonstrator for True Random Number Generation," *IEEE Transactions on Electron Devices*, vol. 64, no. 5, pp. 2185–2192, 2017.

[3] D. L. Scharfetter and H. Gummel, "Large-signal analysis of a silicon Read diode oscillator," *IEEE Trans. Electron Dev.*, vol. ED-16(1), pp. 64–77, 1969.

[4] M. Rudan, *Physics of Semiconductor Devices*. Springer, 2018.

[5] J. Vigo-Aguia and H. Ramos, "A variable-step Numerov method for the numerical solution of the Schrödinger equation," *Journal of Mathematical Chemistry*, vol. 37, no. 3, pp. 255–262, 2005.

[6] M. Rudan, A. Gnudi, E. Gnani, S. Reggiani, and G. Baccarani, "Improving the Accuracy of the Schrödinger-Poisson Solution in CNWs and CNTs," in *IEEE International Conference on Simulation of Semiconductor Processes and Devices (SISPAD)*, Bologna, September 2010, pp. 307–310.

[7] T. Graen and H. Grubmüller, "NuSol–Numerical solver for the 3D stationary nuclear Schrödinger equation," *Computer Physics Communications*, vol. 198, pp. 169–178, 2016.